

Ribose-Modified Purine Nucleosides as Ribonucleotide Reductase Inhibitors. Synthesis, Antitumor Activity, and Molecular Modeling of N^6 -Substituted 3'-C-Methyladenosine Derivatives

Loredana Cappellacci,[†] Palmarisa Franchetti,[†] Patrizia Vita,[†] Riccardo Petrelli,[†] Antonio Lavecchia,[‡] Hiremagalur N. Jayaram,[§] Philipp Saiko,^{||} Geraldine Graser,^{||} Thomas Szekeres,^{||} and Mario Grifantini^{*†}

Dipartimento di Scienze Chimiche, Università di Camerino, 62032 Camerino, Italy, Dipartimento di Chimica Farmaceutica e Tossicologica, Università di Napoli "Federico II", 80131 Napoli, Italy, Department of Biochemistry and Molecular Biology, Indiana University School of Medicine and Richard Roudebush VA Medical Center, Indianapolis, Indiana 46202, Clinical Institute of Medical and Chemical Laboratory Diagnostics, Medical University of Vienna, 1090 Vienna, Austria

Received February 27, 2008

A series of cycloalkyl, bicycloalkyl, aryl, and heteroaryl N^6 -substituted derivatives of the antitumor agent 3'-C-methyladenosine (3'-Me-Ado), an inhibitor of the α Rnr1 subunit of mammalian ribonucleotide reductase (RR), were synthesized. The cytotoxicity of these compounds was evaluated against a panel of human leukemia and carcinoma cell lines and compared to that of some corresponding N^6 -substituted adenosine analogues. N^6 -cycloalkyl-3'-C-methylribonucleosides **2–7** and N^6 -phenyl analogue **8** were found to inhibit the proliferation of K562 leukemia cells. N^6 -(\pm)-endo-2-norbornyl-3'-C-methyladenosine (**7**) was found to be the most cytotoxic compound, with GI_{50} values slightly higher than that of 3'-Me-Ado against K562 and carcinoma cell lines and 2.7 fold higher cytotoxicity against human promyelocytic leukemia HL-60 cells. The SAR study confirms that an unsubstituted N^6 -amino group is essential for optimal cytotoxicity of 3'-Me-Ado against both K562 and carcinoma cell lines. Computational studies, carried out on the eukaryotic α subunit (Rnr1) of RR from *Saccharomyces cerevisiae* were performed to rationalize the observed structure–activity relationships.

Introduction

Nucleoside analogues such as 2-chloro-2'-deoxyadenosine (cladribine, CldA),^a 9- β -D-arabinofuranosyl-2-fluoroadenine (as phosphate, fludarabine, FaraAMP), 1- β -D-arabinofuranosylcytosine (araC), and 2'-deoxy-2',2'-difluorocytidine (gemcitabine, dFdC) are drugs used in oncology in the treatment of both solid tumors and hematological malignancies.¹ These anticancer nucleosides act as antimetabolites after metabolic activation by phosphorylation to the corresponding 5'-di- or 5'-triphosphates. The target enzymes of the metabolized nucleotides are different. 2-Chloro-2'-deoxyadenosine 5'-triphosphate (CldATP) is incorporated into DNA by DNA polymerase and also potently inhibits ribonucleotide reductase (RR);² fludarabine 5'-triphosphate, (FaraATP) is incorporated into both DNA and RNA, causing inhibition of DNA and RNA polymerases. Moreover, FaraATP inhibits RR as well as DNA ligase¹ and DNA primase.² AraC

5'-triphosphate (araCTP) is incorporated into DNA and induces apoptosis.³ Gemcitabine 5'-diphosphate (dFdCDP) is a very potent inhibitor of RR, and its corresponding 5'-triphosphate (dFdCTP) inhibits DNA polymerase.⁴ Gemcitabine is widely used for treatment of pancreatic and nonsmall cell lung cancers.⁵ Recently, clofarabine {2-chloro-9-(2-deoxy-2-fluoro- β -D-arabinofuranosyl)adenine [clofarex, Cl-F(\dagger)-dAdo]} has been approved for use against pediatric leukemias in both the United States and in the European Union. Clofarabine proved to be a potent inhibitor of both DNA polymerase I and RR.⁶

New sugar-modified cytosine nucleosides, such as (2'S)-2'-deoxy-2'-C-methylcytidine (SMDC), 1-(2-deoxy-2-methylene- β -D-erythro-pentofuranosyl)cytosine (DMDC), 1-(2-C-cyano-2-deoxy-1- β -D-arabino-pentofuranosyl)cytosine (CNDAC), and 1-(3-C-ethynyl- β -D-ribo-pentofuranosyl)cytosine (ECyd) were found to be antitumor agents.⁷ The triphosphate derivative of SMDC is a potent inhibitor of several DNA polymerases. DMDC, as 5'-diphosphate, could be a mechanism-based inhibitor of RR, while its 5'-triphosphate derivative inhibits DNA polymerases. The antitumor activity of CNDAC might be due to the ability of its 5'-triphosphate to inhibit DNA polymerase α and to induce DNA strand breaks. The target enzyme responsible for the cytotoxicity of ECyd seems to be RNA polymerase.

In our continuous efforts in the identification of nucleoside analogues as chemotherapeutic agents that could act by interaction with target enzymes in DNA/RNA biosynthesis, we became interested in the C-branched ribosyl nucleosides endowed with antitumor activity. Recently, we reported that 3'-C-methyladenosine (3'-Me-Ado) is a mechanism-based RR inhibitor endowed with a significant antitumor activity against a panel of human leukemia and carcinoma cell lines.⁸ From structure–activity relationship studies, it was found that the substitution

* To whom correspondence should be addressed. Phone: +39-0737-402233. Fax: +39-0737-637345. E-mail: mario.grifantini@unicam.it.

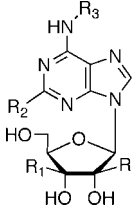
[†] Dipartimento di Scienze Chimiche, Università di Camerino.

[‡] Dipartimento di Chimica Farmaceutica e Tossicologica, Università di Napoli "Federico II".

[§] Department of Biochemistry and Molecular Biology, Indiana University School of Medicine and Richard Roudebush VA Medical Center.

^{||} Clinical Institute of Medical and Chemical laboratory Diagnostics, Medical University of Vienna.

^a Abbreviations: CldA, 2-chloro-2'-deoxyadenosine; FaraAMP, 9- β -D-arabinofuranosyl-2-fluoroadenine 5'-phosphate; dFdC, 2'-deoxy-2',2'-difluorocytidine; Cl-F(\dagger)-dAdo, 2-chloro-9-(2-deoxy-2-fluoro- β -D-arabinofuranosyl)adenine; SMDC, (2'S)-2'-deoxy-2'-C-methylcytidine; DMDC, 1-(2-deoxy-2-methylene- β -D-erythro-pentofuranosyl)cytosine; CNDAC, 1-(2-C-cyano-2-deoxy-1- β -D-arabino-pentofuranosyl)cytosine; ECyd, 1-(3-C-ethynyl- β -D-ribo-pentofuranosyl)cytosine; CPA, N^6 -cyclopentyladenosine; CHA, N^6 -cyclohexyladenosine; CCPA, 2-chloro- N^6 -cyclopentyladenosine; PhA, N^6 -phenyladenosine; BnA, N^6 -benzyladenosine; FMA, N^6 -(2-furanylmethyl)adenosine; TMA, N^6 -(2-thienylmethyl)adenosine; MRS 1334, 1,4-dihydro-2-methyl-6-phenyl-4-(phenylethynyl)-3,5-pyridine-dicarboxylic acid 3-ethyl-5-[(3-nitrophenyl)methyl] ester; DP, diphosphate.

Table 1. In Vitro Activities of Nucleosides 2–21 Against Human Myelogenous Leukemia K562, Human Colon Adenocarcinoma CaCo-2, Human Colon Carcinoma HT-29, and Human Breast Carcinoma MCF-7 Cell Lines


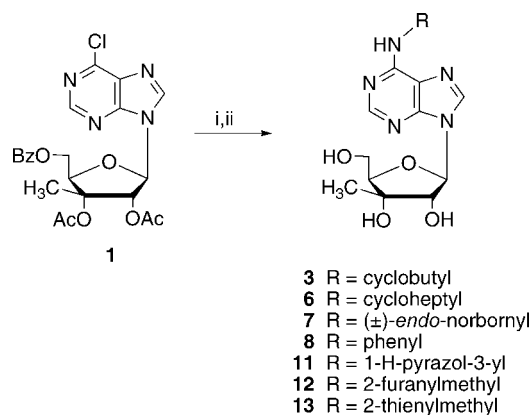
compd	R	R ₁	R ₂	R ₃	GI ₅₀ (μM) ^a			
					K562	CaCo-2	HT-29	MCF-7
2	H	CH ₃	H	cyclopropyl	73	>250	>250	>250
3	H	CH ₃	H	cyclobutyl	246	>250	>250	>250
4	H	CH ₃	H	cyclopentyl	145	>250	>250	>250
5	H	CH ₃	H	cyclohexyl	50	223	>250	>250
6	H	CH ₃	H	cycloheptyl	83	>250	106	200
7	H	CH ₃	H	(±)-endo-2-norbornyl	32.5	56	65.8	56
8	H	CH ₃	H	phenyl	98	246	137	207
9	H	CH ₃	H	benzyl	>250	>250	>250	>250
10	H	CH ₃	Cl	cyclopentyl	>250	>250	>250	>250
11	H	CH ₃	H	1-pyrazol-3-yl	>250	>250	>250	>250
12	H	CH ₃	H	2-furanylmethyl	>250	>250	>250	>250
13	H	CH ₃	H	2-thienylmethyl	>250	>250	>250	>250
14CPA	H	H	H	cyclopentyl	>250	>250	>250	>250
15CCPA	H	H	Cl	cyclopentyl	>250	>250	>250	>250
16CHA	H	H	H	cyclohexyl	>250	>250	>250	>250
17 (±)-ENBA	H	H	H	(±)-endo-2-norbornyl	116	>250	>250	>250
18PhA	H	H	H	phenyl	>250	>250	>250	>250
19BnA	H	H	H	benzyl	4.6	7.4	22.3	61
20FMA	H	H	H	2-furanylmethyl	3.3	45.6	60.2	45.6
21TMA	H	H	H	2-thienylmethyl	3.1	3.3	53.4	51.5
3'-Me-Ado	H	CH ₃	H	H	9.4	23.2	26.1	22.4
2'-Me-Ado ⁸	CH ₃	H	H	H	16	>100	>100	>100
gemcitabine					0.32	0.18	0.03	0.01

^a GI₅₀ values represent the drug concentration required to inhibit cancer cell replication by 50%. Compounds were tested up to a concentration of 250 μM.

of a hydrogen atom of the amino group at the 6-position of the nucleobase in 3'-Me-Ado with a methyl or cyclopropyl group, the introduction of a chlorine atom at the 2-position, or the shifting of the methyl group from the 3'-C position to the other C-positions of the ribose ring results in a decrease or loss of activity, such as for 2'-C-methyl-adenosine (2'-Me-Ado), which showed a lower cytotoxicity than 3'-Me-Ado and reduced ability to inhibit RR.⁸ Further studies confirmed that the structure of 3'-Me-Ado is crucial for the antitumor activity of this type of ribose-modified nucleosides.⁹ In fact, the substitution of adenine in 3'-Me-Ado with other purinic and pyrimidinic nucleobases or the inversion of configuration of the OH group at the 2'-position such as in 3'-Me-araA induces the loss or a significant decrease in cytotoxicity in both human leukemia and carcinoma cell lines. However, by a survey of the literature, we noticed that several adenosine derivatives monosubstituted at the N⁶-position with cycloalkyl, aryl, heterocyclic, or benzyl groups demonstrated significant antitumor activity.¹⁰ N⁶-Benzyladenosine (BnA) is the most interesting compound showing activity against human promyelocytic HL-60 leukemia cells and ability to trigger apoptosis through caspase inhibition.¹¹ Recently, some BnA derivatives with high cytotoxic activity against various cancer cell lines have been reported.¹² These findings prompted us to investigate new derivatives of 3'-Me-Ado substituted at the N⁶-amino group with a series of cycloalkyl, aryl, arylalkyl, or heteroaryl groups.

Chemistry. The 3'-C-ribose-modified purine nucleosides 3, 6–8, and 11–13 were obtained by nucleophilic displacement of the 6-chlorine atom in the protected ribofuranoside **1**⁸ with cycloalkyl, aryl, arylalkyl or heteroaryl amines followed by the sugar deblocking in basic conditions (Scheme 1). Compounds

Scheme 1^a



^a Reagents and conditions: i) R-NH₂, EtOH reflux; ii) NH₃/MeOH, r.t.

2, 4, 5, 9, 10, 14–21 and reference compounds 3'-Me-Ado and 2'-me-Ado were synthesized as reported in the literature.^{8,13–15}

Biological Evaluation and Discussion

The antitumor activity of the new 3'-C-methyladenosine derivatives substituted in the N⁶-amino group was evaluated in human myelogenous leukemia K562, human colon adenocarcinoma CaCo-2, human colon carcinoma HT-29, and human breast carcinoma MCF-7 cell lines, following previously reported methods (Table 1).^{8,9} The cytotoxicity of a series of nonmethylated analogues, namely cyclopentyladenosine (CPA), cyclohexyladenosine (CHA), 2-chloro-cyclopentyladenosine (CCPA), N⁶-phenyladenosine (PhA), N⁶-benzyladenosine (BnA), N⁶-(2-furanylmethyl)adenosine (FMA), and N⁶-(2-thienylm-

ethyl)adenosine (TMA), was also determined. 3'-Me-Ado 2'-Me-Ado and gemcitabine were used as reference compounds. Most of these compounds have not been previously evaluated against these types of tumor cell lines.

Among the *N*⁶-cycloalkylamino-3'-*C*-methyl nucleosides, cyclohexyl derivative **5** showed cell growth inhibition with a GI₅₀ (50% of growth inhibitory concentration) of 50 μM against K562 cells, while the cycloheptyl analogue **6** showed moderate activity against HT-29 and MCF-7 cells in addition to K562. The size of the cycloalkyl substituent influences antileukemic activity as follows: cyclohexyl > cyclopropyl ≥ cycloheptyl > cyclopentyl > cyclobutyl. The 2-chloro modification in 3'-Me-CPA (compound **10**) resulted in the loss of activity.

The *N*⁶-(±)-*endo*-2-norbornyl derivative **7** proved to be the most active compound, showing cytotoxicity against all tested tumor cells with GI₅₀ values ranging from 32.5 to 65.8 μM, turning out to be only 2.5–3.5-fold less active than 3'-Me-Ado, while the *N*⁶-phenyl analogue **8** showed a moderate to marginal activity. In general, these nucleosides proved to be less active than gemcitabine. However, it should be pointed out that the cytotoxicity of gemcitabine is due not only to the inhibition of RR through its metabolite dFdCDP but also to the ability of dFdCTP to inhibit DNA polymerase;⁴ furthermore, the mechanism of RR inhibition of this drug is different from that of other known RR suicide inhibitors.¹⁶

The GI₅₀ values of the *N*⁶-substituted derivatives of 3'-Me-Ado could be dependent on their cellular uptake properties and/or metabolic activation. The lack of or very modest cytotoxicity showed by some compounds may be the result of their inability to be activated by the appropriate enzymes to the monophosphate level and then up to the di and/or triphosphate levels.

It is interesting that among the *N*⁶-substituted adenosine derivatives, BnA (**19**), FMA (**20**), and TMA (**21**) displayed a significant activity similar to that of 3'-Me-Ado against all tested cell lines. On the contrary, *N*⁶-cyclopentyl-, *N*⁶-cyclohexyl-, and *N*⁶-phenyladenosine analogues were inactive against these types of tumor cells despite these nucleosides being previously found to be active or to induce apoptosis in HL-60 cells.^{10b,17,18} The *N*⁶-(±)-*endo*-2-norbornyl analogue **17** showed moderate activity only against K562 cells with a GI₅₀ value of 116 μM, 3.5 fold higher than that of corresponding 3'-*C*-methyl analogue **7**. From the cytotoxicity data, it may be stated that the 3'-*C*-methyl modification at the ribose moiety of **19–21** (compounds **9**, **12**, and **13**) abolishes activity.

Although the cytotoxicity of *N*⁶-benzyladenosine and its bioisosters **20** and **21** was already known, their mechanism of action is not well understood. It has been suggested that the intracellular phosphorylation of BnA is necessary for its cytotoxicity,¹⁸ and in the active form, this compound and similar nucleosides could be able to inhibit several human protein kinases among which CDKs. From a survey of the literature, we found that *N*⁶-benzyladenosine, *N*⁶-(2-furanylmethyl)adenosine, and *N*⁶-(2-thienylmethyl)adenosine behave as agonists at human A₃ adenosine receptor subtype with K_i of 41.3, 22, and 60 nM, respectively.¹⁹ In recent reports, it was well-documented that adenosine A₃ receptor agonists are able to inhibit cell growth and/or induce apoptosis in various tumors both in vitro and in vivo.²⁰ These findings prompted us to hypothesize that the cytotoxicity of compounds **19–21** may be due to the stimulation of adenosine A₃ receptor in target cells. To check this hypothesis, we carried out an experiment to verify if the tumor growth inhibitory effect of *N*⁶-benzyladenosine could be antagonized by MRS 1334 {1,4-dihydro-2-methyl-6-phenyl-4-(phenylethynyl)-3,5-pyridine-dicarboxylic acid 3-ethyl-

Table 2. Effect of MRS 1334 in Reversing Activity of *N*⁶-Benzyladenosine in Human Myelogenous Leukemia K562 Cells^a

duration of treatment (h)	MRS 1334 (μM)	<i>N</i> ⁶ -benzyladenosine ^b			
		GI ₅₀ (μM)			
		2 μM	4 μM	6 μM	average
48	0.1	3.62	3.81	4.30	3.91
48	1.0	4.24	3.89	4.39	4.17
72	0.1	3.09	3.07	2.60	2.92
72	1.0	2.60	3.09	3.07	2.92

^a K562 cells (2000 cells/0.1 mL) growing in logarithmic phase were cultured in 96-well plates in duplicates and incubated at 37 °C in 95% air and 5% CO₂. Twenty-four hours later, saline and 0.1 μM or 1.0 μM MRS 1334 was added and further incubated for 30 min. At the end of 30 min, 2, 4, or 6 μM *N*⁶-benzyladenosine was added, mixed, and incubated for 48 or 72 h. To the wells 20 μL of MTS reagent was added and further incubated for 3 h and the absorbance was read at 490 nm. Fifty percent growth inhibitory concentration (GI₅₀) was calculated based on the observed growth inhibition. ^b GI₅₀ value of *N*⁶-benzyladenosine without the pretreatment with MRS 1334 was 4.6 μM.

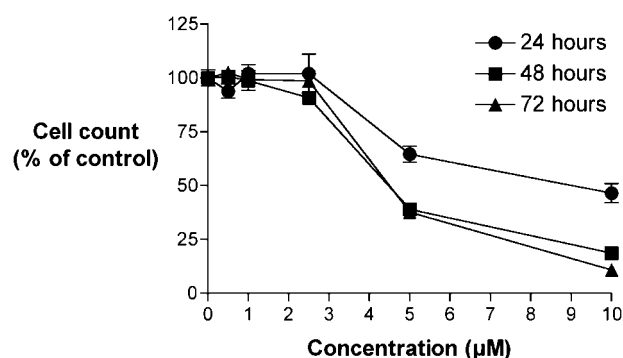


Figure 1. Growth inhibition assay in HL-60 cells after treatment with *N*⁶-(±)-*endo*-norbornyl-3'-*C*-methyladenosine.

5-[(3-nitrophenyl)methyl] ester}, a selective adenosine A₃ receptor antagonist.²¹

K562 cells were pretreated with MRS 1334 (0.1 and 1 μM) for 30 min followed by addition of BnA (2, 4, or 6 μM) and then incubated for 48 or 72 h at 37 °C. GI₅₀ values reported in Table 2 show that the cell growth inhibition exhibited by BnA was not reversed or modified by MRS 1334 treatment. Thus, the cytotoxicity of BnA does not appear to be related to the ability of this compound to stimulate A₃ adenosine receptor. Therefore, the inactivity of 3'-*C*-methyl-*N*⁶-benzyladenosine cannot be attributed to the lower affinity at A₃ AR induced by the 3'-*C*-methyl modification.²² Further studies are needed to identify the biological target(s) of *N*⁶-benzyladenosine.

To confirm that *N*⁶-substituted derivatives of 3'-Me-Ado that showed antitumor activity retain the ability to inhibit the RR, the effect of nucleosides **7** and **8** on cellular RR was evaluated by measuring the level of intracellular deoxyribonucleoside triphosphate pools in HL-60 human promyelocytic leukemia cells before and after treatment with each compound. This indirect method has previously been utilized to evaluate RR inhibition in tumor cells owing to the poor stability of the human enzyme after purification.^{8,23} In HL-60 cells, the cytostatic effect of *N*⁶-(±)-*endo*-norbornyl derivative (**7**) proved to be higher than that of 3'-Me-Ado (GI₅₀ 4.5 and 11⁸ μM, respectively) but lower than that of gemcitabine (GI₅₀ 0.33 μM), while the *N*⁶-phenyl analogue **8** was found to be less active (GI₅₀ 37 μM) (Figures 1 and 2).

Treatment of HL-60 cells with 3'-*C*-methyl-*N*⁶-(±)-*endo*-norbornyladenosine significantly depleted intracellular dATP pools (Figure 3). Incubation for 24 h with 2.5, 5, and 10 μM of

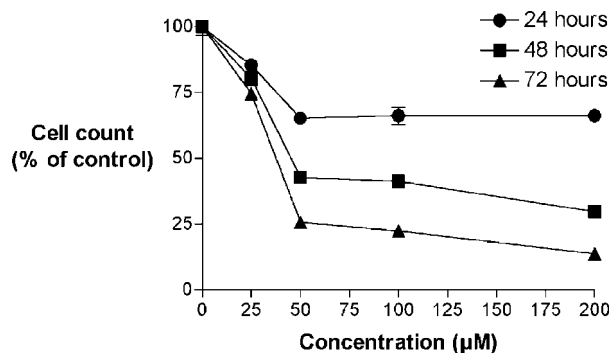


Figure 2. Growth inhibition assay in HL-60 cells after treatment with N^6 -phenyl-3'-*C*-methyladenosine.

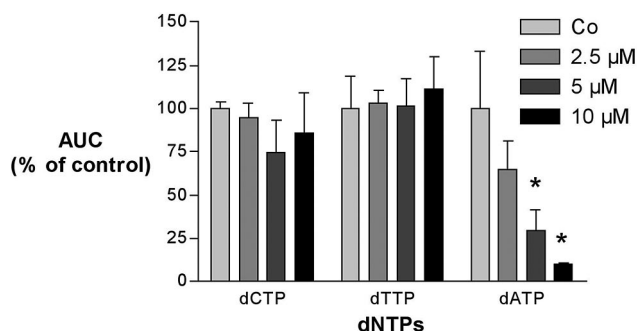


Figure 3. Concentration of dNTP pools in HL-60 cells after treatment with N^6 -(\pm)-endo-norbornyl-3'-*C*-methyladenosine. Values marked with an asterisk (*) are significantly different from the control ($P < 0.05$).

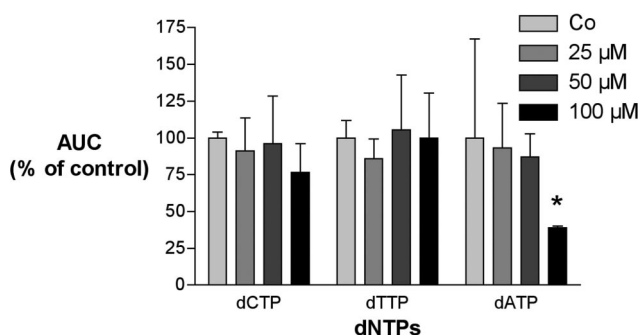


Figure 4. Concentration of dNTP pools in HL-60 cells after treatment with N^6 -phenyl-3'-*C*-methyladenosine. Value marked with an asterisk (*) is significantly different from the control ($P < 0.05$).

7 decreased dATP pools to 65%, 28%, and 10% of control values, respectively. A decrease of dATP pools was observed also with N^6 -phenyl analogue **8** (Figure 4), albeit at higher concentrations. Changes in intracellular dCTP and dTTP concentrations were not significant. Intracellular dGTP pools were below the detection limit of the method used. The fact that intracellular dCTP and dTTP concentrations were not changed is not surprising because other nucleosides that behave as RR inhibitors are able to induce only the depletion of dATP.^{23a} In a similar experiment, 40 nM of gemcitabine decreased intracellular dCTP and dATP pools to 6.1% and 13.9% of control values, respectively.⁸ These findings confirm that also N^6 -substituted derivatives of 3'-*Me*-Ado behave as RR inhibitors.

Molecular Modeling

To explain why 3'-*Me*-Ado has a higher antitumor activity compared to that of 2'-*C*-methyl analogue (2'-*Me*-Ado), as

previously reported by us,⁸ and why the N^6 -substitution in 3'-*C*-methyladenosine induces a decrease of the antitumor activity (with the exception of N^6 -(\pm)-endo-norbornyl derivative **7** in HL-60 cells), we carried out a docking study to elucidate the hypothetical binding mode of 3'-*Me*-Ado, 2'-*Me*-Ado, and N^6 -substituted 3'-*Me*-Ado analogues **7–9**, **12**, and **13** at the RR recognition site. To this end, molecular models were built using the recently solved crystal structure of the eukaryotic α subunit (Rnr1) of RR from *Saccharomyces cerevisiae* complexed with the effector–substrate pair deoxyguanosine triphosphate - (dGTP)–adenosine diphosphate (ADP) (PDB code: 2CVX).²⁴ Although the antitumor activity of our compounds was evaluated on human cell lines, the use of the crystal structure of eukaryotic Rnr1 from *Saccharomyces cerevisiae* for docking studies is justified by the fact that the human RR structure is unavailable and that human and yeast Rnr1 share 66% sequence identity and 83% sequence similarity. The GOLD 3.1 program was used to carry out docking experiments²⁵ because in several studies it yielded better performances when compared to similar programs.²⁶ An analysis of principles and methods adopted by GOLD for energy calculations, conformational search and clustering, and energy ranking is briefly presented in the Experimental Section, whereas a fully detailed description may be found elsewhere.²⁷

It is known that for inhibiting RR, the nucleoside analogues must to be first intracellularly converted to their corresponding 5'-diphosphates. So, our ligands were docked into the RR binding pocket as 5'-diphosphate metabolites (3'-*Me*-ADP, 2'-*Me*-ADP, and diphosphates of compounds **7–9**, **12**, and **13**). The X-ray crystal structure of RR showed six water molecules directly involved in the formation of H-bonds that bridge ADP to the enzyme (W5, W9, W18, W144, W163, and W214).²⁴ To reproduce the observed binding mode of ADP, it was necessary to include all six water molecules in the docking experiments (see Experimental Section for details).

As a validation of the accuracy of the docking program GOLD, the root-mean-square deviation (rmsd) between the top-ranking conformation of ADP predicted by GOLD (fitness score = 111 kJ/mol) and the enzyme-bound conformation of ADP from 2CWX (Figure 5a) was calculated. Given the low rmsd between the experimental and calculated ADP structure (0.36 Å), it was reasonable to expect that GOLD could produce viable docking conformations of the remaining ligands in our study. Furthermore, the H-bonds predicted by GOLD for ADP were virtually identical to those found in the crystallographic ADP/RR complex, as anticipated by the high value of external H-bond (58.8), a GOLD measure for determining the H-bonding interaction between the docked ligand and the protein target. Figure 5b compares the crystallographically observed position of ADP in the RR binding site with the docking result for ADP using all six water molecules.

An in-depth look at the conformer population of 3'-*Me*-ADP generated during the docking simulations into the RR active site revealed that a convergent binding mode was largely adopted. The corresponding result was ranked with the best GOLD fitness score (98.5 kJ/mol) and was found 3 times in 50 independent docking runs. The ligand was found to be in the same location as ADP in the crystal structure. As illustrated in Figure 6a, the $N^{\epsilon 2}$ atom of Q288, which belongs to loop 2, H-bonds to the N1 atom of the adenine. The N3 and N6 atoms on the adenine participate in a second-sphere H-bond, via two water molecules (Wat214 and Wat18, respectively), with the enzyme. The N3 atom of the base also accepts an H-bond from the NH backbone of G247. The 2'-OH of the ribose H-bonds

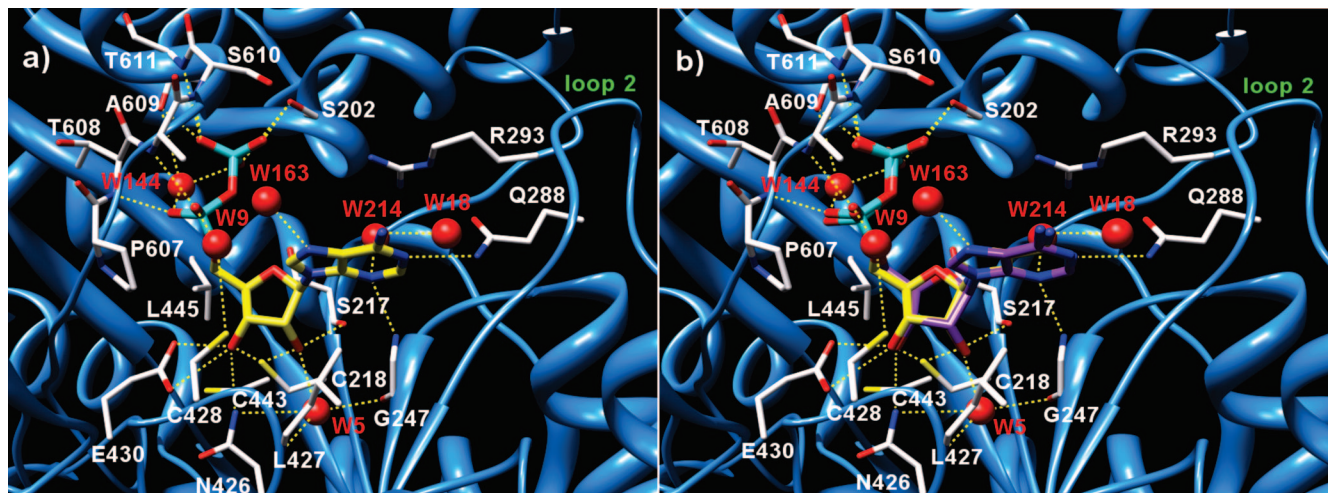


Figure 5. (a) Catalytic-site interactions in the reported crystal structure of the RR-ADP complex (PDB code: 2CVX). The residues involved in H-bonding to ADP (yellow) are also indicated, with their residue type and sequence numbers written in white. Structural water molecules are represented as red balls. H-bonds are symbolized with dashed yellow lines. (b) Crystallographically observed binding mode of ADP (yellow) at the enzyme binding site and GOLD docked binding mode of ADP (purple) in docking experiments carried out with six water molecules placed in the binding site.

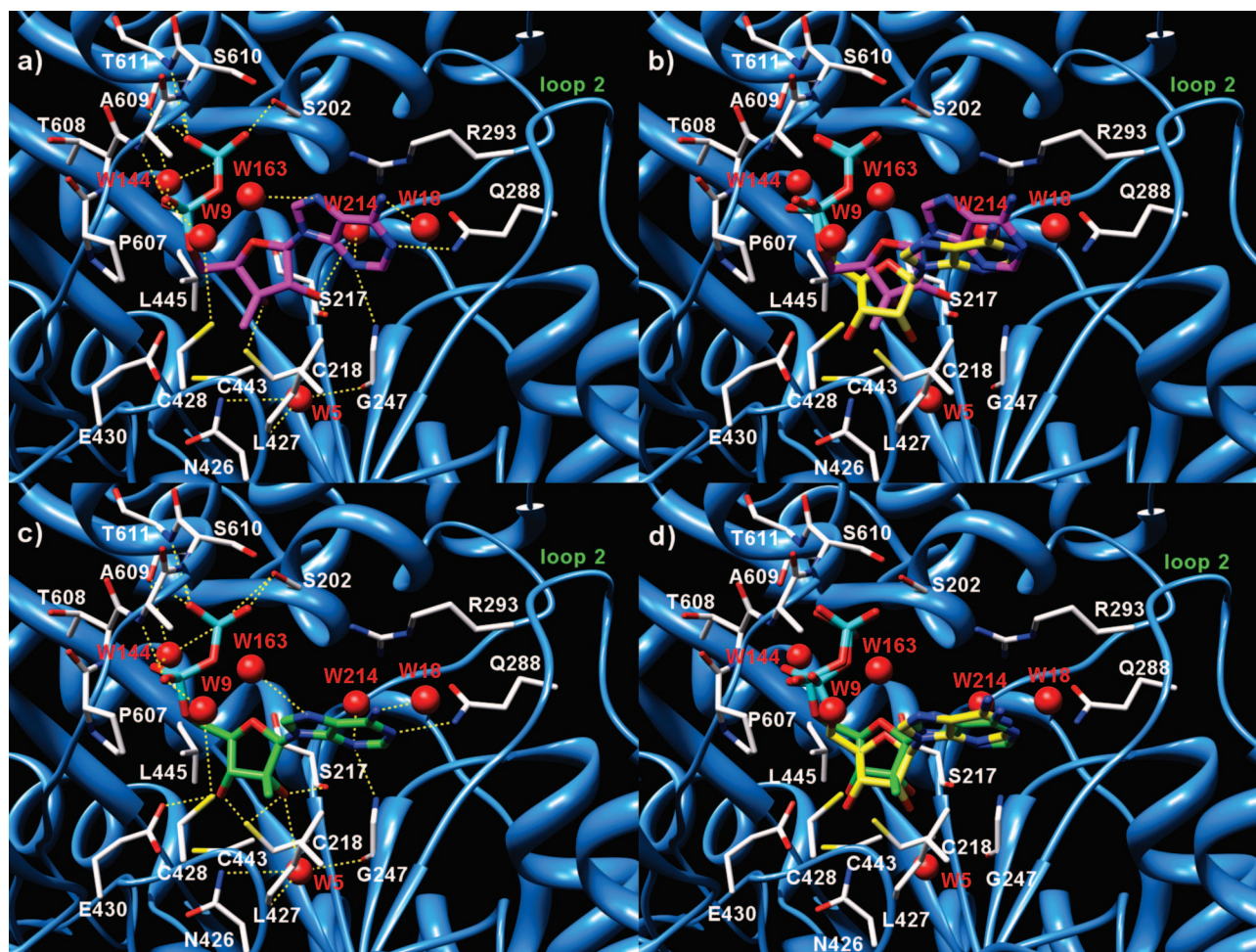


Figure 6. (a) Docked structure of 3'-Me-ADP (magenta) in the RR active site. The residues involved in H-bonding to 3'-Me-ADP are also indicated, with their residue type and sequence numbers written in white. Structural water molecules are represented as red balls. H-bonds are symbolized with dashed yellow lines. (b) Superimposition of the docked structure of 3'-Me-ADP (magenta) on the crystallographic enzyme-bound conformation of ADP (yellow) within the RR active site. (c) Docked structure of 2'-Me-ADP (green) in the RR active site. (d) Superimposition of the docked structure of 2'-Me-ADP (green) on the crystallographic enzyme-bound conformation of ADP (yellow) within the RR active site.

to the S217 C=O oxygen as well as to the conserved water molecule Wat214, whereas the 3'-OH forms a H-bond with the γ atom of C218. The α phosphate of the ligand binds to the

NH backbone of T608 and A609, whereas the β phosphate binds to the NH backbone of S610, T611, and S202 as well as to the OH of S202 side chain. Wat9 and Wat144 contribute to further

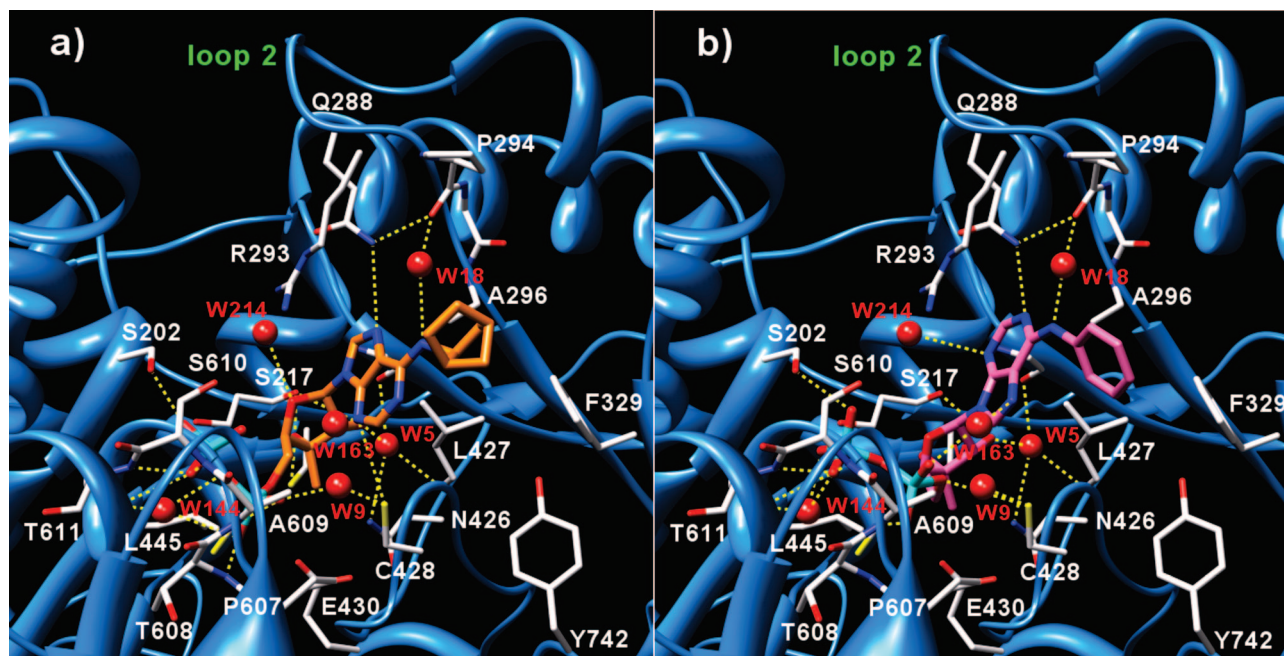


Figure 7. Docked structure of norbornyl derivative **7-DP** (orange, (a)) and phenyl derivative **8-DP** (pink, (b)) in the RR active site.

stabilize the network of H-bonds formed between the ligand diphosphate and the enzyme.

Although 3'-Me-ADP differs from ADP only by the presence of one methyl at 3' position of the ribose ring, it adopts a different conformation when binding to RR. In the RR/dGTP(2'-deoxyguanosine-5'-triphosphate)/ADP complex (Figure 5a), the 2' and 3' OH of the ribose are near the catalytic N426, E430, and C428, where the thiyl radical is generated on Rnr1 by a series of coupled electron and proton transfers,²⁸ and C218 of the reduced catalytic redox pair (C218 and C443). Moreover, a water molecule (Wat5) is found to bind the 2' OH of the ribose, the amide nitrogen of L427, the side chain of N426, and the carbonyl of G247. In contrast, in the RR/dGTP/3'-Me-ADP complex, both the ribose and the base of the ligand appear to be significantly displaced (rmsd = 6.51 Å) from those of ADP (Figure 6b). A possible reason for these differences in the binding mode of 3'-Me-ADP could be given by the fact that the ribose ring in ADP adopts a 3'-endo conformation, whereas in 3'-Me-ADP it adopts a South (²T₃)-syn conformation in which the 3'-methyl projects toward the catalytic residues C428, E430, and N426, altering the H-bonding pattern of 2'- and 3'-OH of 3'-Me-ADP and RR (see Figures 5a and 6a). So, the presence of 3'-methyl in place of 3'-hydrogen impedes the abstraction of the ligand's 3' hydrogen atom by the thiyl radical generated at C428 by a series of coupled proton and electron transfers from Y183* of Rnr2,²⁹ thus explaining why the 3'-Me-ADP behaves as a mechanism-based inhibitor of the RR.

Docking of 2'-Me-ADP into the RR catalytic pocket resulted in a posing (GOLD fitness score = 99.4 kJ) strongly resembling the one reported for ADP with a rmsd value less than 3.0 Å with respect to the crystallographic pose of ADP (Figure 6d). Likely, this is due to the North (³T₂)-anti conformation of the furanose ring, which corresponds to the 3'-endo one of ADP. As depicted in Figure 6c, with the exclusion of the H-bond between the ligand 3'-OH and the enzyme catalytic N426, all the polar interactions observed in the ADP/RR crystallographic complex were preserved in the 2'-Me-ADP/RR complex. The 2' and 3' OH of the ribose were still close to the catalytic N426, E430, C428, and C218 of the reduced catalytic redox pair of cysteines (C218 and C443). So, 2'-Me-ADP should still function

as a substrate of the enzyme, rationalizing its reduced inhibitory activity against RR.

Docking of **7-DP** and **8-DP** to the RR crystal structure provided well-clustered solutions; the top-ranked results (GOLD fitness scores of 90.5 kJ/mol for **7-DP** and 85.3 kJ/mol for **8-DP**) strongly resembled that previously described for 3'-Me-ADP, except for the adenine nucleus of **7-DP**, which was found rotated by 180°. As shown in Figure 7, the ligands had very strong H-bond networking interactions with RR. In addition, the N⁶-norbornyl and -phenyl substituents of both ligands projected just underneath the loop 2 of the enzyme adapting themselves in a hydrophobic cleft made up residues P294, A296, F329, and Y742. In particular, the phenyl ring of **8-DP** was favorably oriented to establish a π - π stacking interaction with F329 ring. These interactions contribute to further stabilize the inhibitor binding, in agreement with the higher cytotoxic activity showed by compounds **7** and **8**.

In the case of the inactive compounds **9**, **12**, and **13**, the automated docking calculations generated multiple docking poses characterized by quite diverse binding modes and comparable fitness scores. Inspection of the docked structures revealed that many of the top-ranked orientations did not fit properly into the active site. In particular, we noticed that the N⁶-substituent of the ligands projected toward the loop 2 (residues 290–297) of the enzyme. In this respect, crystallographic studies demonstrated that the loop 2 of RR contacts the bases of the effector and the substrate, adopting specific conformations in each effector–substrate complex, which provides specificity.^{24,30} In practice, the binding of a specificity effector rearranges loop 2. This rearrangement moves P294, a residue unique to eukaryotes, out of the catalytic site, accommodating substrate binding. Substrate binding further rearranges loop 2. So, extending the N⁶-substituent by one methylene unit in **9** (benzyl), **12** (furanylmethyl), and **13** (thienylmethyl) largely increases its conformational flexibility, which would generate very unfavorable steric interactions with loop 2, leading to a repositioning of the entire molecule in the RR binding pocket

and concomitant disruption of favorable protein–ligand interactions. This rationalizes the lack of RR inhibitory activity of **9**, **12**, and **13**.

Conclusion

In summary, a series of cycloalkyl, bicycloalkyl, phenyl, benzyl, and heteroaryl N^6 -substituted derivatives of the antitumor agent 3'-Me-Ado were synthesized and evaluated for their cytotoxicity against human myelogenous leukemia K562, human colon carcinoma HT-29, human colon adenocarcinoma CaCo-2, and human breast carcinoma MCF-7 cell lines. The cycloalkyl N^6 -substituted 3'-C-methylribonucleosides **2–6** exhibited anticancer activity against K562 cells. The antitumor activity of these derivatives appears to be modulated by the ring size. The N^6 -substitution with a cyclopropyl, cyclohexyl, or cycloheptyl ring provided the most active compounds; however, their cytotoxicity was lower than that of 3'-Me-Ado. The N^6 -(±)-endo-2-norbornyl derivative **7** proved to be the most cytotoxic compound against K562 and carcinoma cell lines with GI₅₀ values slightly higher than that of 3'-Me-Ado and displayed 2.7 fold higher cytotoxicity than 3'-Me-Ado against human promyelocytic leukemia HL-60 cells. The corresponding N^6 -phenyl analogue **8** showed lower cytotoxicity than 3'-Me-Ado against all tested cell lines. These results confirm that an unsubstituted N^6 -amino group is essential for optimal cytotoxicity of 3'-Me-Ado against both human leukemia K562 and carcinoma cell lines.

Nucleosides **7** and **8** significantly depleted dATP pools in HL-60 cells, proving to be RR inhibitors. Docking studies, carried out on the eukaryotic α subunit (Rnr1) of RR from *Saccharomyces cerevisiae*, which shares 66% sequence identity and 83% sequence similarity with human Rnr1, whose structure is unavailable, showed that the activity of N^6 -substituted derivatives of 3'-Me-Ado is largely dependent on the conformational flexibility of the N^6 -substituent with greater flexibility resulting in decreased favorable protein–ligand interactions.

Experimental Section

Chemistry. Elemental analyses were determined on an EA 1108 CHNS-O (Fisons Instruments) analyzer. Thin layer chromatography (TLC) was run on silica gel 60 F₂₅₄ plates (Merck); silica gel 60 (70–230 Merck) for column chromatography was used. Nuclear magnetic resonance ¹H NMR spectra were determined with a Varian Mercury AS400 at 400 MHz. The chemical shift values are expressed in δ values (parts per million) relative to tetramethylsilane as an internal standard. All exchangeable protons were confirmed by addition of D₂O. Mass spectroscopy was carried out on an HP 1100 series instrument. All measurements were performed in the positive ion mode using an atmospheric pressure electrospray ionization (API-ESI). MRS 1334 was purchased from Tocris bioscience. All reagents were purchased from Sigma-Aldrich.

General Procedure for the Amination of **1 into Compounds **3**, **6–8**, and **11–13**.** To a stirred solution of 6-chloro-9H-(3-C-methyl-2,3-di-O-acetyl-5-O-benzoyl- β -D-ribofuranosyl)purine (**1**)⁸ (1.0 mmol) in absolute ethanol (20 mL) and Et₃N (3 mmol) only in the case of compound **7**, the appropriate amine (1.6 mmol) was added. The reaction mixture was refluxed for the time reported below and concentrated in vacuo. The residue was dissolved in methanolic ammonia (10 mL) and stirred at room temperature overnight. The solution was evaporated to dryness and the residue was purified by column chromatography.

N^6 -Cyclobutyl-9H-(3-C-methyl- β -D-ribofuranosyl)adenine (3**).** Reaction of **1** with cyclobutylamine at reflux for 1.5 h followed by deprotection and chromatography on a silica gel column (CHCl₃–MeOH, 95:5) gave **3** as a white solid (87% yield). ¹H NMR (DMSO-*d*₆): δ 1.28 (s, 3H, CH₃), 1.65 (m, 2H, cyclobutyl), 2.10–2.22 (2m, 4H, cyclobutyl), 3.52 (m, 1H, H-5'), 3.65 (m, 1H,

H-5'), 3.85 (t, J = 2.6 Hz, 1H, H-4'), 4.42 (t, J = 7.5 Hz, 1H, H-2'), 4.70 (m, 1H, NHCH), 4.82 (s, 1H, OH-3'), 5.40 (d, J = 6.8 Hz, 1H, OH-2'), 5.80 (d, J = 8.1 Hz, 1H, H-1'), 5.88 (dd, J = 3.0, 8.1 Hz, 1H, OH-5'), 8.15 (s and d, 2H, H-2, NH), 8.35 (s, 1H, H-8). MS: m/z 336.4 [M + H]⁺. Anal. (C₁₅H₂₁N₅O₄) C, H, N.

N^6 -Cycloheptyl-9H-(3-C-methyl- β -D-ribofuranosyl)adenine (6**).** Reaction of **1** with cycloheptylamine at reflux for 2 h followed by deprotection and chromatography on a silica gel column (CHCl₃–MeOH, 95:5) gave **6** as a white solid (80% yield). ¹H NMR (DMSO-*d*₆): δ 1.26 (s, 3H, CH₃), 1.40–1.66 (2m, 10H, cycloheptyl), 1.86 (m, 2H, cycloheptyl), 3.52 (m, 1H, H-5'), 3.62 (m, 1H, H-5'), 3.86 (t, J = 2.6 Hz, 1H, H-4'), 4.25 (m, 1H, NHCH), 4.40 (d, J = 8.1 Hz, 1H, H-2'), 4.88 (s, 1H, OH-3'), 5.40 (d, J = 6.8 Hz, 1H, OH-2'), 5.80 (d, J = 7.7 Hz, 1H, H-1'), 6.0 (dd, J = 3.0, 8.1 Hz, 1H, OH-5'), 7.75 (d, J = 7.7 Hz, 1H, NH), 8.15 (s, 1H, H-2), 8.32 (s, 1H, H-8). MS: m/z 378.5 [M + H]⁺. Anal. (C₁₈H₂₇N₅O₄) C, H, N.

N^6 -(±)-endo-Norbornyl-9H-(3-C-methyl- β -D-ribofuranosyl)adenine (7**).** Reaction of **1** with (±)-endo-2-norbornylamine hydrochloride (2 mmol) and Et₃N (3 mmol) for 7 h followed by deprotection gave **7**, which was purified by chromatography on a silica gel column (CHCl₃–MeOH, 95:5) as a white solid (93% yield). ¹H NMR (DMSO-*d*₆): δ 1.25 (m, 3H, norbornyl), 1.28 (s, 3H, CH₃), 1.43 (m, 3H, norbornyl), 1.60 (m, 1H, norbornyl), 1.90 (m, 1H, norbornyl), 2.15 (br s, 1H, norbornyl), 2.52 (s, 1H, norbornyl), 3.55, 3.65 (2m, 2H, H-5'), 3.86 (br s, 1H, H-4'), 4.34 (m, 1H, NHCH), 4.44 (t, J = 7.4 Hz, 1H, H-2'), 4.83 (s, 1H, OH-3'), 5.40 (dd, J = 2.1, 6.8 Hz, 1H, OH-2'), 5.82 (dd, J = 3.0, 8.1 Hz, 1H, H-1'), 5.9 (dd, J = 3.0, 8.1 Hz, 1H, OH-5'), 7.85 (br s, 1H, NH), 8.18 (s, 1H, H-2), 8.30 (s, 1H, H-8). MS: m/z 376.4 [M + H]⁺. Anal. (C₁₈H₂₅N₅O₄) C, H, N.

N^6 -Phenyl-9H-(3-C-methyl- β -D-ribofuranosyl)adenine (8**).** Reaction of **1** with phenylamine for 4.5 h followed by deprotection and chromatography on a silica gel column (CHCl₃–MeOH, 94:6) gave **8** as a white solid (65% yield). ¹H NMR (400) (DMSO-*d*₆): δ 1.30 (s, 3H, CH₃), 3.52 (m, 1H, H-5'), 3.65 (m, 1H, H-5'), 3.90 (t, J = 2.8 Hz, 1H, H-4'), 4.45 (t, J = 7.1 Hz, 1H, H-2'), 4.90 (s, 1H, OH-3'), 5.47 (d, J = 6.6 Hz, 1H, OH-2'), 5.67 (dd, J = 3.8, 7.1 Hz, 1H, OH-5'), 5.90 (d, J = 8.1 Hz, 1H, H-1'), 7.05 (t, J = 7.5 Hz, 1H, arom), 7.32 (t, J = 7.9 Hz, 2H, arom), 7.90 (d, J = 7.7 Hz, 2H, arom), 8.38 (s, 1H, H-2), 8.50 (s, 1H, H-8), 10.0 (s, 1H, NH). MS: m/z 358.4 [M + H]⁺. Anal. (C₁₇H₁₉N₅O₄) C, H, N.

N^6 -(3-Pyrazolyl)-9H-(3-C-methyl- β -D-ribofuranosyl)adenine (11**).** Reaction of **1** with 3-aminopyrazole for 3 days followed by deprotection and chromatography on a silica gel column (CHCl₃–MeOH, 90:10) gave **11** as a white solid (61% yield). ¹H NMR (DMSO-*d*₆): δ 1.30 (s, 3H, CH₃), 3.55 (m, 1H, H-5'), 3.65 (m, 1H, H-5'), 3.88 (s, 1H, H-4'), 4.45 (t, J = 6.8 Hz, 1H, H-2'), 4.86 (s, 1H, OH-3'), 5.45 (d, J = 6.4 Hz, 1H, OH-2'), 5.68 (br s, 1H, OH-5'), 5.90 (d, J = 7.7 Hz, 1H, H-1'), 6.70 (br s, 1H, arom), 6.65 (br s, 1H, arom), 8.32 (s, 1H, H-2), 8.48 (s, 1H, H-8), 9.90 (br s, 1H, NH), 12.38 (br s, 1H, NH). MS: m/z 348.3 [M + H]⁺. Anal. (C₁₄H₁₇N₇O₄) C, H, N.

N^6 -(2-Furanylmethyl)-9H-(3-C-methyl- β -D-ribofuranosyl)adenine (12**).** Reaction of **1** with 2-furfurylamine for 4.5 h followed by deprotection and chromatography on a silica gel column (CHCl₃–MeOH, 94:6) gave **12** as a white solid (93% yield). ¹H NMR (DMSO-*d*₆): δ 1.30 (s, 3H, CH₃), 3.55 (m, 1H, H-5'), 3.65 (m, 1H, H-5'), 3.86 (t, J = 2.6 Hz, 1H, H-4'), 4.42 (t, J = 7.1 Hz, 1H, H-2'), 4.68 (br s, 2H, CH₂NH), 4.82 (s, 1H, OH-3'), 5.40 (d, J = 6.8 Hz, 1H, OH-2'), 5.80 (dd, J = 3.4, 8.1 Hz, 1H, OH-5'), 5.82 (d, J = 7.7 Hz, 1H, H-1'), 6.20 (d, J = 3.0 Hz, 1H, arom), 6.35 (dd, J = 1.7, 3.4 Hz, 1H, arom), 7.52 (d, J = 1.7 Hz, 1H, arom), 8.20 (s, 1H, H-2), 8.32 (br s, 1H, NH), 8.34 (s, 1H, H-8), MS: m/z 362.3 [M + H]⁺. Anal. (C₁₆H₁₉N₅O₅) C, H, N.

N^6 -(2-Thienylmethyl)-9H-(3-C-methyl- β -D-ribofuranosyl)adenine (13**).** Reaction of **1** with 2-thiophenemethylamine for 6 h followed by deprotection and chromatography on a silica gel column (CHCl₃–MeOH, 93:7) gave **13** as a white solid (72% yield). ¹H NMR (DMSO-*d*₆): δ 1.30 (s, 3H, CH₃), 3.55 (m, 1H, H-5'), 3.65 (m, 1H, H-5'), 3.86 (t, J = 2.6 Hz, 1H, H-4'), 4.42 (t, J = 7.3 Hz,

1H, H-2'), 4.82 (s and br s, 3H, OH-3', CH₂NH), 5.40 (d, $J = 6.8$ Hz, 1H, OH-2'), 5.80 (dd, $J = 3.2, 7.9$ Hz, 1H, OH-5'), 5.82 (d, $J = 8.1$ Hz, 1H, H-1'), 6.90 (dd, $J = 3.4, 5.1$ Hz, 1H, arom), 7.0 (d, $J = 2.6$ Hz, 1H, arom), 7.32 (d, $J = 5.1$ Hz, 1H, arom), 8.22 (s, 1H, H-2), 8.38 (s, 1H, H-8), 8.58 (br s, 1H, NH). MS: m/z 362.3 [M + H]⁺. Anal. (C₁₆H₁₉N₅O₄S) C, H, N.

Computational Chemistry. Molecular modeling and graphics manipulations were performed using the molecular operating environment (MOE)³¹ and UCSF-CHIMERA software packages³² running on a Silicon Graphics Tezro R16000 workstation. Energy minimizations were realized by employing the AMBER 9 program,³³ selecting the Cornell et al. force field.³⁴

Ligand and Protein Setup. The core structures of compounds 2'-Me-Ado, 3'-Me-Ado, 7-9, 12, and 13 were retrieved from the Cambridge Structural Database (CSD)³⁵ and modified using standard bond lengths and bond angles of the MOE fragment library. Geometry optimizations were accomplished with the MMFF94X force field,³⁶ available within MOE.

The crystal structure of the eukaryotic α subunit (Rnr1) of RR from *Saccharomyces cerevisiae* complexed with the effector-substrate pair dGTP-ADP (PDB code: 2CVX),²⁴ recovered from Brookhaven Protein Database,^{37,38} was used for the docking experiments. Hydrogen atoms were added to ADP, dGTP, water molecules, and protein. Partial atomic charges for ADP, dGTP, and the crystallographically determined water molecules were computed by MOE using the AMBER99 force field. All heavy atoms were then fixed and hydrogen atoms were minimized using the AMBER99 force field and a constant dielectric of 1, terminating at a gradient of 0.001 kcal mol⁻¹·Å⁻¹. The bound ADP, dGTP, and the water molecules were then removed, leaving in the active site only the six water molecules (W5, W9, W18, W144, W163, and W214)²⁴ that interact directly with ADP.

Docking Simulations. Docking of 2'-Me-ADP, 3'-Me-ADP, 7-9-DP, 12-DP and 13-DP to RR was performed with GOLD 3.1 version,²⁵ which uses a genetic algorithm for determining the docking modes of ligands and proteins. An advantage of GOLD over other docking methods is the program's ability to account for some rotational protein flexibility as well as full ligand flexibility. Specifically, OH groups of Ser, Thr, and Tyr and amino groups of Lys are allowed to rotate during docking to optimize H-bonding to the ligand. GOLD requires a user-defined binding site. It searches for a cavity within the defined area and considers all the solvent-accessible atoms in that area as active-site atoms. The fitness score function implemented in GOLD (GOLDScore) is made up of four components that account for protein-ligand binding energy: protein-ligand H-bond energy (external H-bond), protein-ligand van der Waals energy (external vdW), ligand internal vdW energy (internal vdW), and ligand torsional strain energy (internal torsion). Parameters used in the fitness function (H-bond energies, atom radii and polarizabilities, torsion potentials, H-bond directionalities, and so forth) are taken from the GOLD parameter file. The fitness score is taken as the negative of the sum of the energy terms, so larger fitness scores indicated better bindings. The fitness function has been optimized for the prediction of ligand binding positions rather than the prediction of binding affinities, although some correlation with the latter can be also found. The protein input file may be the entire protein structure or a part of it comprising only the residues that are in the region of the ligand binding site. In the present study, GOLD was allowed to calculate interaction energies within a sphere of a 13 Å radius centered on the S7' atom of C218 in the RR structure. Fifty independent docking runs were performed for each docking experiment, using standard default settings with a population size of 100, a maximum number of 300000 operations, and a mutation and crossover rate of 95. After docking, the best generated 10 solutions of each ligand were ranked according to their fitness scores calculated by the GOLDScore function.

To determine the minimum number and combination of water molecules required, water molecules were then systematically removed, giving active sites with various combinations of 6, 5,

4, 3, 2, 1, and 0 water molecules in place, and ADP was redocked each time. These experiments showed that the position of ADP in the active site could be reliably reproduced by docking to a protein with all six water molecules (W5, W9, W18, W144, W163, and W214)²⁴ in the site (Figure 5a). Dockings using less than six water molecules were much less successful, giving rise to solutions in which the ADP was docked in various inverted, rotated, and distorted conformations.

Energy Refinement of the Ligand/Enzyme Complexes. To eliminate any residual geometric strain, the obtained complexes were energy minimized for 5000 steps using combined steepest descent and conjugate gradient methods until a convergence value of 0.001 kcal/mol·Å. Upon minimization, the protein backbone atoms and the six water molecules were held fixed. The geometry optimizations were performed using the SANDER module in the AMBER suite of programs, employing the Cornell et al. force field to assign parameters for the standard amino acids. General AMBER force field (GAFF) parameters were assigned to ligands, while the partial charges were calculated using the AM1-BCC method as implemented in the ANTECHAMBER suite of AMBER.

Cells and Culture. The cell lines human myelogenous leukemia K562, human promyelocytic leukemia HL-60, human colon carcinoma HT-29, human colon adenocarcinoma CaCo-2, and human breast carcinoma MCF-7 were obtained from the American type Culture Collection (ATCC, Manassas, VA). K562 and HL-60 cells were maintained in RPMI 1640 medium (Gibco/Life Technologies, Gaithersburg, MD) containing 10% heat-inactivated fetal bovine serum (FBS) (Atlanta Biologicals, Atlanta, GA) and 10000 U/L penicillin and 50 mg/L streptomycin. HT-29, CaCo2, and MCF-7 cells were maintained in MEM with Earl's balanced salts, 10% FBS, penicillin, and streptomycin as above. Logarithmically growing HT-29, CaCo2, and MCF-7 cells were incubated with 0.05% trypsin containing 1 mM EDTA at 37 °C for about 5 min until cells were nonadherent and formed a single cell suspension. Trypsin activity was neutralized by adding 20-fold excess of the serum-containing medium. Cells were cultured at 37 °C in an atmosphere of air and 5% CO₂.

Antitumor Assay. Cytotoxicity assays were conducted by tetrazolium reduction of 3-(4,5-dimethylthiazol-2-yl)-5-(3-carboxymethoxyphenyl)-2-(4-sulfophenyl)-2H-tetrazolium (MTS) with *N*-methylphenazonium methyl sulfate (PMS) (CellTiter Assay, Promega, Madison, WI). Logarithmically growing cells were plated in 0.1 mL aliquots in 96-well microtiter plates. Cells were plated at an initial density of about 5000 cells/mL and allowed to acclimatize for 24 h. Cell suspensions were treated with various dilutions of compounds in triplicate, mixed well, and allowed to incubate for 48 h at 37 °C in an atmosphere of air and 5% CO₂. To the cell suspension was added 20 μ L of tetrazolium reagent, the mixture was incubated for 3 h at 37 °C in an atmosphere of air and 5% CO₂, and absorbance at 490 nm was read by microplate reader. Control plates with serial dilutions of cell types were counted as a control for the assay. In all cases, controls indicated a linear response versus cell number, $R^2 \geq 0.99$.

Analysis of Intracellular dNTP Pools by High Performance Liquid Chromatography (HPLC). Logarithmically growing HL-60 cells (0.5×10^6 per ml) were incubated with 2.5, 5, and 10 μ M 7 or 25, 50, and 100 μ M 8 for 24 h. Afterward, 5×10^7 cells were separated for the extraction of dNTPs according to the method described by Garrett and Santi.³⁹ Cells were centrifuged at 1800 rpm for 5 min and then resuspended in 100 μ L phosphate-buffered saline. In this suspension, cells were lysed by addition of 10 μ L of trichloroacetic acid and the mixture was vortexed for 1 min. The lysate was rested on ice for 30 min and then the protein was separated by centrifugation at 15000 rpm for 10 min in an Eppendorf microcentrifuge. The supernatant was removed and neutralized by adding 1.1 vol of Freon containing 0.5 M tri-*n*-octylamine. Aliquots of 100 μ L were periodated by adding 30 μ L of 4 M methylamine solution and 10 μ L of sodium periodate solution (concentration: 100 mg/mL).

After incubation at 37 °C for 30 min, the reaction was stopped by adding 5 μ L of 1 M rhamnose solution. The extracted dNTPs were measured using a Merck "La Chrom" high-performance liquid chromatography (HPLC) system (Merck, Darmstadt, Germany) equipped with L-7200 autosampler, L-7100 pump, L-7400 UV detector, and D-7000 interface. Detection time was set at 80 min, with the detector operating on 280 nm for 40 min and then switched to 260 nm for another 40 min. Samples were eluted with a 3.2 mol/L ammonium phosphate buffer, pH 3.4 (pH adjusted by addition of 3.2 mM H₃PO₄), containing 2% acetonitrile using a 4.6 \times 250 mm Partisil 10 SAX analytical column (Whatman Ltd., Kent, UK). Separation was performed at constant ambient temperature with a flow rate of 2 mL/min. The concentration of dNTPs was calculated as percent of total area under the curve for each sample.

Acknowledgment. The research was supported by the Italian MIUR (PRIN 2006) and by Veterans Affairs Merit Review Award (USA) (to H.N.J.).

Supporting Information Available: Analysis data. This material is available free of charge via the Internet at <http://pubs.acs.org>.

References

- Parker, W. B.; Secrist, J. A., III; Waud, W. R. Purine Nucleoside Antimetabolites in Development for the Treatment of Cancer. *Curr. Opin. Invest. Drugs* **2004**, *5*, 592–596.
- Tsimberidou, A. M.; Alvarado, Y.; Giles, F. J. Evolving Role of Ribonucleotide Reductase Inhibitors in Hematologic Malignancies. *Expert Rev. Anticancer Ther.* **2002**, *2*, 437–448, and references cited therein.
- Sreenivasan, Y.; Sarkar, A.; Manna, S. K. Mechanism of Cytosine Arabinoside-mediated Apoptosis: Role of Rel A (p65) Dephosphorylation. *Oncogene* **2003**, *22*, 4356–4369.
- Jacobs, A. D. Gemcitabine-Based Therapy in Pancreas Cancer. Gemcitabine-Docetaxel and Other Novel Combinations. *Cancer* **2002**, *95*, 923–927, and references cited therein.
- (a) Burkes, R. L.; Shepherd, F. A. Gemcitabine in the Treatment of Non-small-cell Lung Cancer. *Ann. Oncol.* **1995**, *6* (Suppl. 3), S57–60. (b) King, R. S. Gemcitabine. New First-line Therapy for Pancreatic Cancer. *Cancer Pract.* **1996**, *4*, 353–354.
- Bonate, P. L.; Arthaud, L.; Cantrell, W. R., Jr.; Stephenson, K.; Secrist, J. A., III; Weitman, S. Discovery and Development of Clofarabine: a Nucleoside Analogue for Treating Cancer. *Nat. Rev. Drug Discov.* **2006**, *5*, 855–863.
- Matsuda, A.; Sasaki, T. Antitumor activity of sugar-modified cytosine nucleosides. *Cancer Sci.* **2004**, *95*, 105–111.
- Franchetti, P.; Cappellacci, L.; Pasqualini, M.; Petrelli, R.; Vita, P.; Jayaram, H. N.; Horvath, Z.; Szekeres, T.; Grifantini, M. Antitumor Activity of C-Methyl- β -D-ribofuranosyladenine Nucleoside Ribonucleotide Reductase Inhibitors. *J. Med. Chem.* **2005**, *48*, 4983–4989.
- Cappellacci, L.; Franchetti, P.; Petrelli, R.; Riccioni, S.; Vita, P.; Jayaram, H. N.; Grifantini, M. Purine and Pyrimidine Nucleoside Analogs of 3'-C-Methyladenosine as Antitumor Agents. *Collect. Czech. Chem. Commun.* **2006**, *71*, 1088–1098.
- (a) Colquhoun, A.; Newsholme, E. A. Inhibition of Human Tumour Cell Proliferation by Analogues of Adenosine. *Cell Biochem. Funct.* **1997**, *15*, 135–139. (b) Grindey, G. B.; Divekar, A. Y.; Hakala, M. T. Antitumor Activity of N⁶-Phenyladenosine, and Inhibitor of Adenosine Utilization, in Combination with Related Purine Analogs. *Cancer Res.* **1973**, *33*, 2459–2463.
- (a) Mlejnek, P.; Kuglik, P. Induction of Apoptosis in HL-60 Cells by N⁶-Benzyladenosine. *J. Cell. Biochem.* **2000**, *77*, 6–17. (b) Mlejnek, P. Caspase Inhibition and N⁶-Benzyladenosine-Induced Apoptosis in HL-60 Cells. *J. Cell. Biochem.* **2001**, *83*, 678–689.
- Dolezal, K.; Popa, I.; Hauserová, E.; Spíchal, L.; Chakrabarty, K.; Nová, O.; Krystof, V.; Voller, J.; Holub, J.; Strnad, M. Preparation, Biological Activity and Endogenous Occurrence of N⁶-Benzyladenosine. *Bioorg. Med. Chem.* **2007**, *15*, 3737–3747.
- Lohse, M. J.; Klotz, K.-N.; Schwabe, U.; Cristalli, G.; Vittori, S.; Grifantini, M. 2-Chloro-N⁶-cyclopentyladenosine: a Highly Selective Agonist at A₁ Adenosine Receptors. *Naunyn-Schmiedeberg's Arch. Pharmacol.* **1988**, *337*, 687–689.
- Fleysher, M. H.; Bloch, A.; Hakala, M. T.; Nichol, C. A. Synthesis and Biological Activity of Some New N⁶-Substituted Purine Nucleosides. *J. Med. Chem.* **1969**, *12*, 1056–1061.
- Kissman, H. M.; Weiss, M. J. Kinetin Riboside and Related Nucleosides. *J. Org. Chem.* **1956**, *21*, 1053–1055.
- Pereira, S.; Fernandes, P. A.; Ramos, M. J. Mechanism for Ribonucleotide Reductase Inactivation by the Anticancer Drug Gemcitabine. *J. Comput. Chem.* **2004**, *25*, 1286–1294.
- Thedford, R.; Leyimu, E. O.; Thornton, D. L.; Mehta, R. Cytotoxicity of N⁶-Cycloalkylated Adenine and Adenosine Analogs to Mouse Hepatoma Cells. *Expl. Cell. Biol.* **1989**, *57*, 53–59.
- Mlejnek, P.; Dolezal, P. Apoptosis Induced by N⁶-Substituted Derivatives of Adenosine is Related to Intracellular Accumulation of Corresponding Mononucleotides in HL-60 Cells. *Toxicol. in Vitro* **2005**, *19*, 985–990.
- Gao, Z.-G.; Blaustein, J. B.; Gross, A. S.; Melman, N.; Jacobson, K. A. N⁶-Substituted Adenosine Derivatives: Selectivity, Efficacy, and Species Differences at A₃ Adenosine Receptors. *Biochem. Pharmacol.* **2003**, *65*, 1675–1684.
- (a) Fishman, P.; Bar-Yehuda, S.; Ardon, E.; Rath-Wolfson, L.; Barrer, F.; Ochaion, A.; Madi, L. Targeting the A₃ Adenosine Receptor for Cancer Therapy: Inhibition of Prostate Carcinoma Cell Growth by A₃AR Agonist. *Anticancer Res.* **2003**, *23*, 2077–2083. (b) Chung, H.; Jung, J. Y.; Cho, S. D.; Hong, K. A.; Kim, H. J.; Shin, D. H.; Kim, H.; Kim, H. O.; Shin, D. H.; Lee, H. W.; Jeong, L. S.; Kong, G. The Antitumor Effect of LJ-529, a Novel Agonist to A₃ Adenosine Receptor, in both Estrogen Receptor-Positive and Estrogen Receptor-Negative Human Breast Cancers. *Mol. Cancer Ther.* **2006**, *5*, 685–692. (c) Nakamura, K.; Yoshikawa, N.; Yamaguchi, Y.; Kagota, S.; Shinozuka, K.; Kunitomo, M. Antitumor Effect of Cordycepin (3'-Deoxyadenosine) on Mouse Melanoma and Lung Carcinoma Cells Involves Adenosine A₃ Receptor Stimulation. *Anticancer Res.* **2006**, *26*, 43–47.
- Li, A.-H.; Moro, S.; Melman, N.; Ji, X.-D.; Jacobson, K. A. Structure-Activity Relationships and Molecular Modeling of 3,5-Diacyl-2,4-dialkylpyridine Derivatives as Selective A₃ Adenosine Receptor Antagonists. *J. Med. Chem.* **1998**, *41*, 3186–3201.
- Cappellacci, L.; Franchetti, P.; Pasqualini, M.; Petrelli, R.; Vita, P.; Lavecchia, A.; Novellino, E.; Costa, B.; Martini, C.; Klotz, K.-N.; Grifantini, M. Synthesis, Biological Evaluation and Molecular Modeling of Ribose-Modified Adenosine Analogues as Adenosine Receptor Agonists. *J. Med. Chem.* **2005**, *48*, 1550–1562.
- (a) Coucke, P. A.; Decoster, L. A.; Li, Y. X.; Cottin, E.; Chen, X.; Sun, L. Q.; Stern, S.; Paschoud, N.; Denekamp, J. The Ribonucleoside Diphosphate Reductase Inhibitor (E)-2'-Deoxy-(fluoromethylene)cytidine as a Cytotoxic Radiosensitizer, in Vitro. *Cancer Res.* **1999**, *59*, 5219–5226. (b) Johns, D. G.; Gao, W. Y. Selective Depletion of DNA Precursors: An Evolving Strategy for Potentiation of Dideoxynucleoside Activity Against Human Immunodeficiency Virus. *Biochem. Pharmacol.* **1998**, *55*, 1551–1556. (c) Fox, R. M. Changes in Deoxynucleoside Triphosphate Pools Induced by Inhibitors and Modulators of Ribonucleotide Reductase. *Pharmacol. Ther.* **1985**, *30*, 31–42. (d) Reichard, P. Ribonucleotide Reductase and Deoxyribonucleotide Pools. *Basic Life Sci.* **1985**, *31*, 33–45. (e) Szekeres, T.; Fritzer-Szekeres, M.; Elford, H. L. The Enzyme Ribonucleotide Reductase: Target for Antitumor and Anti-HIV Therapy. *Crit. Rev. Clin. Lab. Sci.* **1997**, *34*, 503–528.
- Xu, H.; Faber, C.; Uchiki, T.; Fairman, J. W.; Racca, J.; Dealwis, C. Structures of Eukaryotic Ribonucleotide Reductase I Provide Insights into dNTP Regulation. *Proc. Natl. Acad. Sci. U.S.A.* **2006**, *103*, 4022–4027.
- Jones, G.; Willett, P.; Glen, R. C.; Leach, A. R.; Taylor, R. Development and Validation of a Genetic Algorithm for Flexible Docking. *J. Mol. Biol.* **1997**, *267*, 727–748.
- (a) Schulz-Gasch, T.; Stahl, M. Binding Site Characteristics in Structure-Based Virtual Screening: Evaluation of Current Docking Tools. *J. Mol. Model.* **2003**, *9*, 47–57. (b) Wang, R.; Lu, Y.; Wang, S. Comparative Evaluation of 11 Scoring Functions for Molecular Docking. *J. Med. Chem.* **2003**, *46*, 2287–2303. (c) Kellenberger, E.; Rodrigo, J.; Muller, P.; Rognan, D. Comparative Evaluation of Eight Docking Tools for Docking and Virtual Screening Accuracy. *Proteins: Struct., Funct., Bioinf.* **2004**, *57*, 225–242.
- Westhead, D. R.; Clark, D. E.; Murray, C. W. A Comparison of Heuristic Search Algorithms for Molecular Docking. *J. Comput.-Aided Mol. Des.* **1997**, *11*, 209–228.
- Mao, S. S.; Holler, T. P.; Yu, G. X.; Bollinger, J. M., Jr.; Booker, S.; Johnston, M. I.; Stubbe, J. Interaction of C225SR1 Mutant Subunit of Ribonucleotide Reductase with R2 and Nucleoside Diphosphates: Tales of a Suicidal Enzyme. *Biochemistry* **1992**, *31*, 9733–9743.
- Stubbe, J.; van der Donk, W. A. Ribonucleotide Reductases: Radical Enzymes with Suicidal Tendencies. *Chem. Biol.* **1995**, *2*, 793–801.
- Larsson, K. M.; Jordan, A.; Eliasson, R.; Reichard, P.; Logan, D. T.; Nordlund, P. Structural Mechanism of Allosteric Substrate Specificity Regulation in a Ribonucleotide Reductase. *Nat. Struct. Mol. Biol.* **2004**, *11*, 1142–1149.
- Molecular Operating Environment (MOE), version 2005.06*; Chemical Computing Group, Inc.: Montreal, Canada, 2005.

- (32) Huang, C. C.; Couch, G. S.; Pettersen, E. F.; Ferrin, T. E. Chimera: An Extensible Molecular Modelling Application Constructed Using Standard Components. *Pac. Symp. Biocomput.* **1996**, *1*, 724. <http://www.cgl.ucsf.edu/chimera>.
- (33) Case, D. A.; Darden, T. A.; Cheatham, T. E., III; Simmerling, C. L.; Wang, J.; Duke, R. E.; Luo, R.; Merz, K. M.; Pearlman, D. A.; Crowley, M.; Walker, R. C.; Zhang, W.; Wang, B.; Hayik, S.; Roitberg, A.; Seabra, G.; Wong, K. F.; Paesani, F.; Wu, X.; Brozell, S.; Tsui, V.; Gohlke, H.; Yang, L.; Tan, C.; Mongan, J.; Hornak, V.; Cui, G.; Beroza, P.; Mathews, D. H.; Schafmeister, C.; Ross, W. S.; Kollman, P. A. *AMBER 9*; University of California, San Francisco, 2006.
- (34) Cornell, W. D.; Cieplak, P.; Bayly, C. I.; Gould, I. R.; Merz, K. M.; Ferguson, D. M.; Spellmeyer, D. C.; Fox, T.; Caldwell, J. W.; Kollman, P. A. A Second Generation Force Field for the Simulation of Proteins, Nucleic Acids, and Organic Molecules. *J. Am. Chem. Soc.* **1995**, *117*, 5179–5197.
- (35) Allen, F. H.; Bellard, S.; Brice, M. D.; Cartwright, B. A.; Doubleday, A.; Higgs, H.; Hummelink, T.; Hummelink-Peters, B. G.; Kennard, O.; Motherwell, W. D. S. The Cambridge Crystallographic Data Center: Computer-Based Search, Retrieval, Analysis and Display of Information. *Acta Crystallogr., Sect. B: Struct. Sci.* **1979**, *35*, 2331–2339.
- (36) (a) Halgren, T. A. Merck Molecular Force Field. I. Basis, Form, Scope, Parameterization, and Performance of MMFF94. *J. Comput. Chem.* **1996**, *17*, 490–512. (b) Halgren, T. A. Merck Molecular Force Field. II. MMFF94 van der Waals and Electrostatic Parameters for Intermolecular Interactions. *J. Comput. Chem.* **1996**, *17*, 520–552. (c) Halgren, T. A. Merck Molecular Force Field. III. Molecular Geometries and Vibrational Parameters for Intermolecular Interactions. *J. Comput. Chem.* **1996**, *17*, 553–586. (d) Halgren, T. A. Merck Molecular Force Field. IV. Conformational Energies and Geometries for MMFF94. *J. Comput. Chem.* **1996**, *17*, 587–615. (e) Halgren, T. A. Merck Molecular Force Field. V. Extension of MMFF94 Using Experimental Data, Additional Computational Data, and Empirical Rules. *J. Comput. Chem.* **1996**, *17*, 616–641.
- (37) Bernstein, F. C.; Koetzle, T. F.; Williams, G. J. B.; Meyer, E. F., Jr.; Brice, M. D.; Rodgers, J. R.; Kennard, O.; Shimanouchi, T.; Tasumi, T. The Protein Data Bank: A Computer Based Archival File for Macromolecular Structures. *J. Mol. Biol.* **1977**, *112*, 535–542.
- (38) Verdonk, M. L.; Cole, J. C.; Hartshorn, M. J.; Murray, C. W.; Taylor, R. D. Improved Protein–Ligand Docking Using Gold. *Proteins: Struct., Funct., Bioinf.* **2003**, *52*, 609–623.
- (39) Garrett, C.; Santi, D. V. A Rapid and Sensitive High Pressure Liquid Chromatography Assay for Deoxyribonucleoside Triphosphates in Cell Extracts. *Anal. Biochem.* **1979**, *99*, 268–273.

JM800205C